

University of Nebraska - Lincoln

DigitalCommons@University of Nebraska - Lincoln

David Sellmyer Publications

Research Papers in Physics and Astronomy

July 1973

Magnetoresistance in Iron and Cobalt to 150 kOe

R.V. Coleman

Department of Physics, University of Virginia, Charlottesville, Virginia

R.C. Morris

Department of Physics, University of Virginia, Charlottesville, Virginia

David J. Sellmyer

University of Nebraska-Lincoln, dsellmyer@unl.edu

Follow this and additional works at: <https://digitalcommons.unl.edu/physicsellmyer>



Part of the [Physics Commons](#)

Coleman, R.V.; Morris, R.C.; and Sellmyer, David J., "Magnetoresistance in Iron and Cobalt to 150 kOe " (1973). *David Sellmyer Publications*. 179.

<https://digitalcommons.unl.edu/physicsellmyer/179>

This Article is brought to you for free and open access by the Research Papers in Physics and Astronomy at DigitalCommons@University of Nebraska - Lincoln. It has been accepted for inclusion in David Sellmyer Publications by an authorized administrator of DigitalCommons@University of Nebraska - Lincoln.

Magnetoresistance in Iron and Cobalt to 150 kOe*†

R. V. Coleman and R. C. Morris

Department of Physics, University of Virginia, Charlottesville, Virginia 22901

D. J. Sellmyer

Department of Metallurgy and Materials Science, Massachusetts Institute of Technology, Cambridge, Massachusetts 02139

and Behlen Laboratory of Physics, ‡ University of Nebraska, Lincoln, Nebraska 68508

(Received 26 December 1972)

Magnetoresistance anisotropy and field dependence have been studied in single crystals of iron and cobalt in fields up to 150 kOe in the temperature range 1–4.2 K. The crystals of iron and cobalt had residual resistance ratios up to ≈ 4600 and ≈ 400 , respectively. The relation $\Delta\rho/\rho_0 = aB^n$ has been studied for both metals and in the case of iron the exponent n approaches values in the range 1.8–1.9 for fields up to 90 kOe and then decreases to the range 1.3–1.5 at 150 kOe. This decrease in the exponent has been observed for all field and current directions measured suggesting that extensive magnetic breakdown may occur. A preliminary measurement on iron to 215 kOe shows n decreasing to less than 1 for some field directions. Cobalt shows saturation behavior for most field and current directions but values of $n > 1$ are observed for certain specific directions. The magnetoresistance rotation curves for iron exhibit sharp minima consistent with narrow bands of open orbits in the $\langle 100 \rangle$ and $\langle 110 \rangle$ directions. Minima are also observed which indicate open orbits in the $\langle 310 \rangle$, $\langle 410 \rangle$, and $\langle 530 \rangle$ directions. The behavior of cobalt suggests open orbits parallel to the basal plane and possibly along the c axis. Both metals show Shubnikov-de Haas oscillations which appear to be related to small pockets of the Fermi surface corresponding to 10^{-3} – 10^{-4} electrons per atom. In iron oscillations with frequencies in the range 1–6.2 MG have been observed while in cobalt three oscillations with frequencies of 1.07, 3.57, and 11.63 MG have been observed. The low-frequency oscillation in cobalt has been studied as a function of angle and indicates that two distinct branches exist as the field is rotated away from the c axis. Oscillations are observed on only one branch at a time and the behavior suggests the possible presence of magnetic breakdown. The data on both iron and cobalt have been compared to models of the Fermi-surface topology in these metals.

I. INTRODUCTION

The 3d transition metals iron and cobalt have been extensively studied from many points of view but the Fermi surface and band structure are still not known with anything like the degree of accuracy which has been attained for many other metals. This has been primarily due to the limited amount of experimental data that give direct information on the Fermi surface and this in turn has been related to the difficulty of obtaining highly perfect single crystals. Two detailed band-structure calculations for ferromagnetic iron^{1,2} have recently been published and a number of calculations also exist for paramagnetic iron.^{3–9} In the case of cobalt^{10,11} several band-structure calculations have been published, although the Fermi surface of cobalt is at present considerably more uncertain than that of iron. The most complete experimental work on iron has been done by Gold *et al.*¹² using the de Haas-van Alphen effect. In addition, preliminary magnetoresistance results on iron have been reported by Reed and Fawcett^{13,14} and by Isin and Coleman.¹⁵ These experiments have provided sufficient data to check a number of predictions from the band-structure calculations, but many points are still unresolved. The experimental situation on cobalt is rapidly improving from that of a few

years ago when no experimental Fermi-surface data were available. Rosenman and Batallan¹⁶ and Anderson and Hudak¹⁷ have reported initial results of de Haas-van Alphen measurements and Reed and Fawcett¹⁴ and Marker *et al.*¹⁸ have reported preliminary results on the magnetoresistance in cobalt. All of these experiments have been severely limited by the quality of the crystals and only relatively small sections of the Fermi surface have been studied so far.

In this paper we report on results of magnetoresistance experiments in which we have extended the range of the applied field to 150 kOe and in a few cases to 215 kOe. We have used crystals grown in the form of "whiskers" which have so far proved to be the most perfect single crystals available for these two metals. The extended field range has certainly helped to clarify many features of the data and we describe the experiments and results below.

II. EXPERIMENTAL METHODS

The iron and cobalt specimens used in the present experiments were prepared by the method of hydrogen reduction of FeCl_2 and CoBr_2 . A standard Vycor combustion tube in a cylindrical furnace was used. Combustion boats filled with the chloride or bromide were placed in the combustion tube in a

position to reach the correct temperature and temperature gradient. Details of this standard method can be found in several review articles.^{19,20} For the growth of iron crystals pure flowing hydrogen was used, while for the growth of cobalt crystals a mixture of argon and hydrogen was used. Iron "whiskers" grow in the temperature range (600–800) °C while cobalt "whiskers" grow in the range (400–600) °C.

These methods of growth by hydrogen reduction are used in order to avoid the problem of defects introduced by phase transitions which occur in both of these metals. For iron, (α - γ), 910 °C; (γ - δ), 1400 °C; mp=1539 °C. For cobalt, (hcp-fcc) 417 °C; mp=1495 °C. In the case of iron the crystals clearly grow in the low-temperature bcc phase and are nearly perfect. The situation for cobalt is less clear. The best specimens appear to grow in a temperature range near or just above the phase transition which suggests that they may grow initially in the hcp phase. On the other hand, specimens which grow in the fcc phase will transform on cooling and a high density of stacking faults may be introduced. In addition, some fraction of the fcc phase may be frozen in and this has in fact been reported by various investigators.^{20,21} The residual resistance ratios [RRR = $R(295 \text{ °K})/R(4.2 \text{ °K})$] for cobalt vary over a wide range even for the same combustion boat and this may reflect a considerable variation in perfection. The best RRR's obtained have been used in the present experiment and were 383, 265, 255, and 204.

In the case of iron the purity and perfection is much higher and specimens with RRR's in the range 1000–5000 can be selected fairly easily. The best RRR used in the present experiments was 4600 and specific RRR's for the various specimens are indicated in the figures. The mean free path in the iron specimens is sufficiently great that the specific domain geometry dominates the resistance at $H=0$ due to the effects of the internal field $B=4\pi M_s=22.02 \text{ kG}$ within each domain at 4.2 °K. This results in a very sharp field dependence of resistance in the low-field region where the crystal is in the multidomain state. An example is shown for the application of a longitudinal field in Fig. 1. In computing the RRR and the magnetoresistance $\Delta\rho/\rho_0 = [\rho(B) - \rho(0)]/\rho(0)$ we have used the value of the resistance at the minimum in the curve of Fig. 1 as the best value of the true zero-field resistance and this should represent an upper limit for the impurity resistance. A similar but much smaller effect is observed in the cobalt specimens and does not constitute a significant correction to the RRR. More extensive details of the contribution to the magnetoresistance due to the domain geometry in iron have been given by Shumate *et al.*²²

The iron specimens have diameters in the range

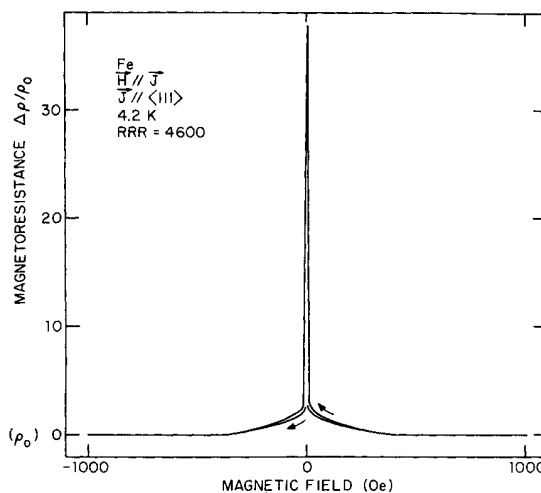


FIG. 1. Low-field longitudinal magnetoresistance for $\langle 111 \rangle$ axial iron whisker. Giant peak near $H=0$ is due to multidomain structure.

200–700 μ and length-to-diameter ratios from 30 to 50. The cobalt whiskers have diameters in the range 30–50 μ and length-to-diameter ratios in the range 50–80. The values of B have been calculated from $B=H+4\pi M_s - DM_s$, where D is the appropriate longitudinal or transverse demagnetizing factor based on the above length-to-diameter ratios. For a number of the field sweeps the samples have been tipped away from the transverse orientation by an angle ϕ and then rotated about the sample axis (current axis). This method has been used to study the angular dependence of the Shubnikov-de Haas oscillations in cobalt. The angular dependence of the demagnetizing factor has then been approximated by $D_\phi = D_T \cos^3 \phi$, where D_T is the transverse demagnetizing factor for the particular specimen. The plots of oscillation number as a function of $1/B$ using this model for the demagnetizing factor all give linear plots at high fields and the frequencies agree with those determined for equivalent field directions measured in the longitudinal field orientation where the demagnetizing factor is negligible ($\sim 100 \text{ Oe}$). In the case of tipping experiments where oscillations can be observed down to very low fields, a deviation from linearity in $1/B$ can be observed for the low-field oscillations. This could be due to an inaccurate value of the demagnetizing factor based on this approximate model, but various checks of the analysis suggest that this cannot account entirely for the deviation. A more likely source would be the rotation of the internal field relative to the external field direction which can increase at low fields.

The resistance measurements have been made using a standard four-lead arrangement formed on circuit boards to which the specimens have been

soldered. The circuit boards are mounted on various rotating sample holders which can be inserted into the vertical-bore solenoids used in these experiments. For magnetic fields up to 80 kOe we have used superconducting solenoids and for fields up to 215 kOe we have used Bitter solenoids at the National Magnet Laboratory. The sample currents have been supplied by highly regulated power supplies and the potentials have been recorded using Keithley microvoltmeters. Most of the measurements have been made in a bath of liquid helium at 4.2 °K while a few have been carried out at temperatures down to 1.1 °K. The lower temperature was observed to improve the resolution of the Shubnikov-de Haas oscillations in some cases, but no substantial new effects were observed at the low temperatures.

III. EXPERIMENTAL MAGNETORESISTANCE RESULTS

Magnetoresistance curves have been recorded in fields up to 150 kOe for both iron and cobalt. Various current axes have been used and the resulting magnetoresistance structure will be described below.

A. Iron

In the case of iron the majority of the more perfect crystals grow with axes along the low-index directions $\langle 100 \rangle$, $\langle 110 \rangle$, and $\langle 111 \rangle$, and typical transverse-rotation curves at 150 kOe are shown for these three current directions in Fig. 2. The observed anisotropy at 150 kOe represents (20–30)% of the total magnetoresistance with relatively sharp minima observed whenever the field direction lies in a $\{100\}$ or a $\{110\}$ plane. Relatively smaller minima are also observed when the field lies in higher-index planes such as $\{310\}$, $\{420\}$, and $\{530\}$. The relevant field sweeps and positions of the minima for the three transverse rotations are shown in the stereo plot of Fig. 3. In the case of the $\langle 111 \rangle$ current axis the transverse-rotation curve at 150 kOe as shown in Fig. 2(c) indicates that the relative depths of the $\langle 112 \rangle$ and $\langle 110 \rangle$ minima are reversed from the identification given in Ref. 15 for a rotation curve recorded at 50 kOe. This reversal is real and appears to be connected with the field dependence of the exponent n which varies with field orientation and in a number of cases produces a reversal in the relative depths of the minima as the field is increased in the range above 50 kOe.

If the crystal axis is tipped away from the transverse orientation most of the minima persist over a fairly large angular range and examples of these rotation plots are shown in Fig. 4 for a $\langle 111 \rangle$ axial crystal. Rotation diagrams for tip angles up to 30° are shown in Fig. 4 and correspond to angles between the current and the magnetic field in the

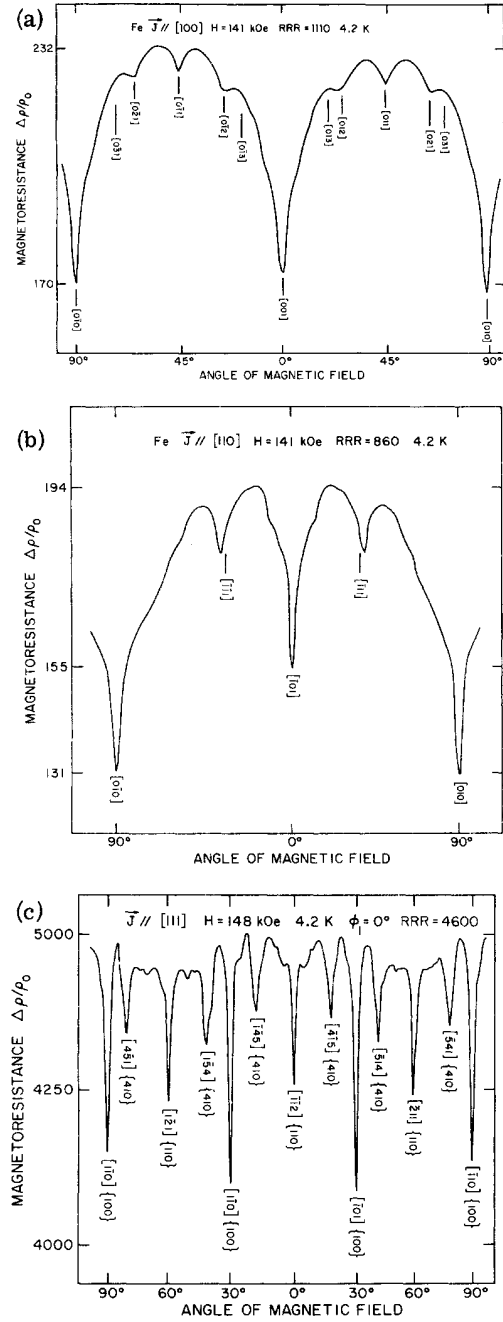


FIG. 2. Transverse-magnetoresistance-rotation curves for iron with current in low-index directions. (a) $[100]$ axial specimen; (b) $[110]$ axial specimen; (c) $[111]$ axial specimen.

range 90° – 60° . The corresponding field sweeps and positions of the minima are shown in the $\langle 111 \rangle$ stereo projection of Fig. 5. The field sweeps are indicated by the circles labeled $\phi_1, \phi_2, \phi_3, \phi_4, \phi_5$. The major minima occur whenever the field lies in a $\{100\}$ or a $\{110\}$ plane and persist over the 30° range of field angles shown here. Relatively

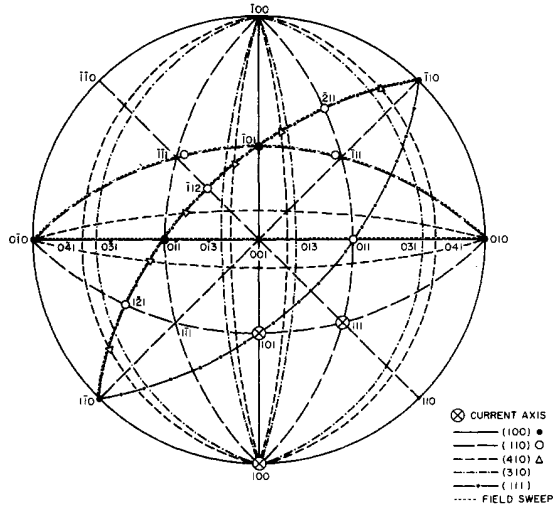


FIG. 3. (001) projection showing current axes and special field directions where sharp minima are observed in the transverse magnetoresistance. Field sweeps for the three low-index current axes are shown. Minima observed when the field lies in (100), (110), and (410) planes are indicated. Minima observed for two different field sweeps coincide at (110) poles and are indicated by \odot .

smaller minima occur when the field lies in (410) planes as shown by the open triangles in Fig. 5. In addition, for field directions near a (100) pole, shallow minima are observed for field directions which lie close to {310} and {530} planes as indicated by the filled triangles and open squares, respectively, in Fig. 5.

The magnetoresistance for all field and current directions measured shows a functional dependence of the form $\Delta\rho/\rho_0 = aB^n$, where n is greater than one. In the intermediate field range, $30 < B < 100$ kG, n approaches the value of 2 expected for a compensated metal, but decreases at higher fields reaching values in the range 1.3–1.5 at 150 kG. The relative values of n vary for field directions corresponding to maxima and minima in the rotation curves, but a substantial decrease in n at higher-field values is observed for all field directions. Examples for comparison are indicated in Figs. 6(a) and 6(b) where log-log plots of $\Delta\rho/\rho_0$ vs B are shown for various field directions. Figure 6(a) shows plots for field directions corresponding to a maximum and a minimum, respectively, in the (111) transverse-rotation curve of Fig. 2(c), while Fig. 6(b) compares the field dependence at the (100) and (110) minima in the (110) rotation curve of Fig. 2(b). We have recently extended the measurements to 215 kOe and the exponent n continues to decrease and becomes less than 1 for several of the field directions corresponding to minima. An example is shown in Fig. 7(b) and details of the

higher-field measurements will be reported in a later publication.

For applied magnetic fields above 90 kOe ($B \sim 100$ kG) Shubnikov-de Haas oscillations are observed

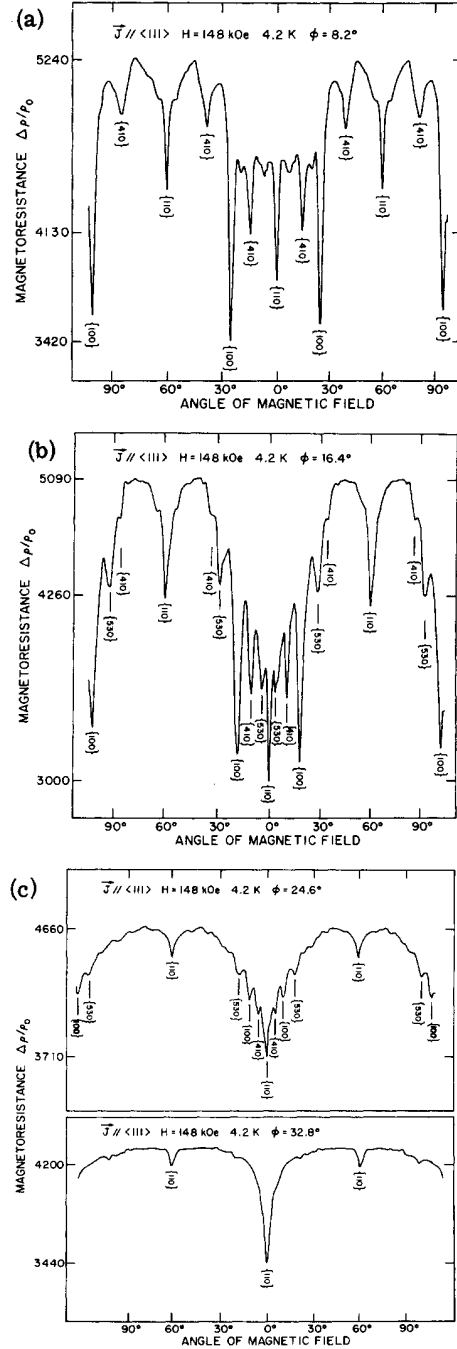


FIG. 4. Magnetoresistance rotation curves obtained by tipping a (111) axial iron specimen away from the transverse orientation by an angle ϕ and rotating about the current axis. (a) $\phi_2 = 8.2^\circ$; (b) $\phi_3 = 16.4^\circ$; (c) $\phi_4 = 24.6^\circ$ and $\phi_5 = 32.8^\circ$.

for a range of field directions. Fawcett²³ has also observed these low-frequency oscillations over a range of field directions in iron whiskers. These are particularly strong for field directions lying in $\{110\}$ planes when the current is along $\langle 111 \rangle$, and examples are shown in Fig. 7(a). These oscillations have been observed for the fields up to 150 kOe at all directions between $\langle 112 \rangle$ and $\langle 541 \rangle$ for the transverse orientation when the current is in a $\langle 111 \rangle$ direction. They also exist over a reasonably large two-dimensional region of field directions as the $\langle 111 \rangle$ axial crystals are tipped away from the transverse orientation. The frequencies of the oscillations observed up to 150 kOe are all close to 1.5 MG.

The more recent experiments in the range 150–215 kOe show oscillations appearing for a number of other field directions in addition to those discussed above. Several of the field directions also show oscillations at two different frequencies in the higher-field range and examples are shown in Fig. 7(b). The figure shows data on a crystal with an axis close to the $\langle 100 \rangle$ direction. The two deep minima show a definite trend toward saturation and exhibit oscillations as indicated by the arrows. The magnetoresistance anisotropy observed at 215 kOe has also increased to approximately 50%. The short period observed at minimum 3 (the circled 3 in the figure) corresponds to a frequency of ~ 4.7 MG, while the long-period oscillations at the minima 1 and 3 correspond to frequencies of 1 and 1.3

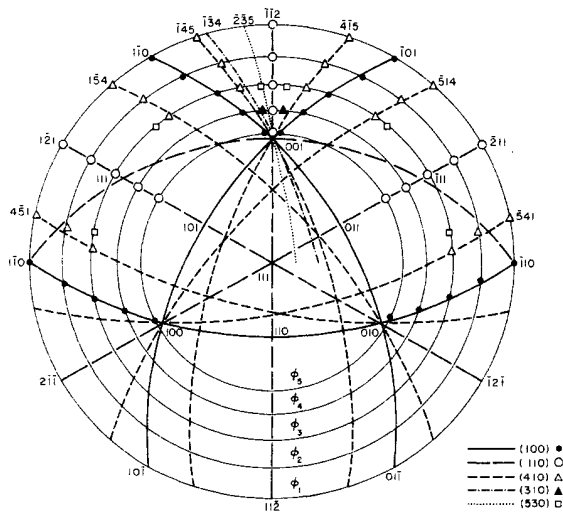


FIG. 5. $\langle 111 \rangle$ projection plot showing field sweeps and positions of minima observed in the magnetoresistance-rotation curves for iron shown in Fig. 4. Relevant low-index planes are also indicated and coded as shown in lower right-hand side. The light solid curves labeled ϕ_1 , ϕ_2 , ϕ_3 , ϕ_4 , and ϕ_5 represent the field sweeps. Data for ϕ_2 – ϕ_5 are shown in Fig. 4.

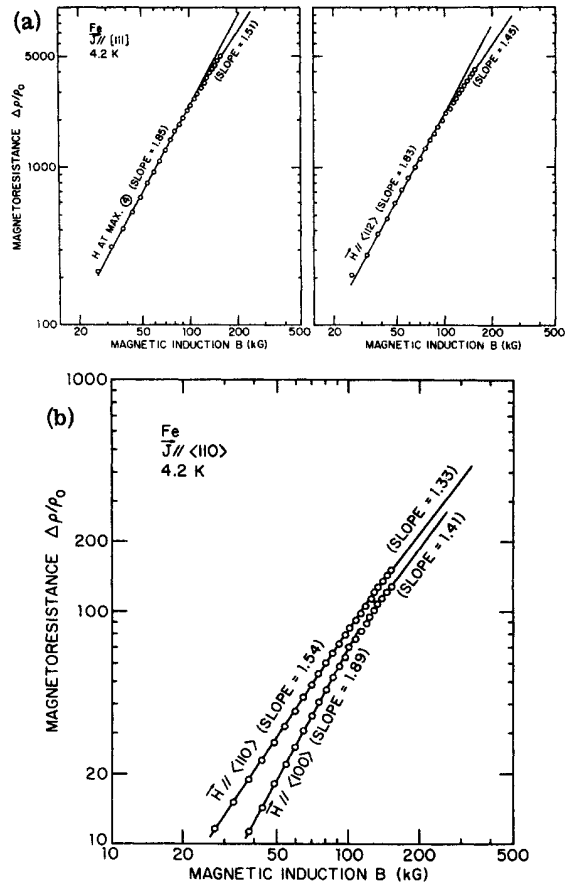


FIG. 6. Log-log plots of the relation $\Delta\rho/\rho_0 = aB^n$ with values of n indicated by the slopes determined from the solid lines. (a) $\langle 111 \rangle$ axial iron specimen in transverse orientation. Maximum at 4 (the circled 4) is indicated in Fig. 7(a). (b) $\langle 110 \rangle$ axial iron specimen in transverse orientation.

MG, respectively. The nonsaturating field direction 5 also shows a weak long-period oscillation corresponding to a frequency of 1.4 MG.

B. Cobalt

Transverse-magnetoresistance-rotation diagrams for three cobalt specimens at 150 kOe are shown in Fig. 8 and correspond to current axes along the c axis, in the basal plane, and between the c axis and basal plane. For field directions lying in the basal plane the rotation diagrams show maxima, while for field directions near the c axis or at large angles to the basal plane the rotation curves show relative minima. For most field directions the exponent n in the functional form $\Delta\rho/\rho_0 = aB^n$ is less than one and the magnetoresistance shows a definite trend toward saturation as shown in curve A of Fig. 8(a). However, when both current and field lie near the basal plane, the coefficient n is greater than one and no trend toward saturation is ob-

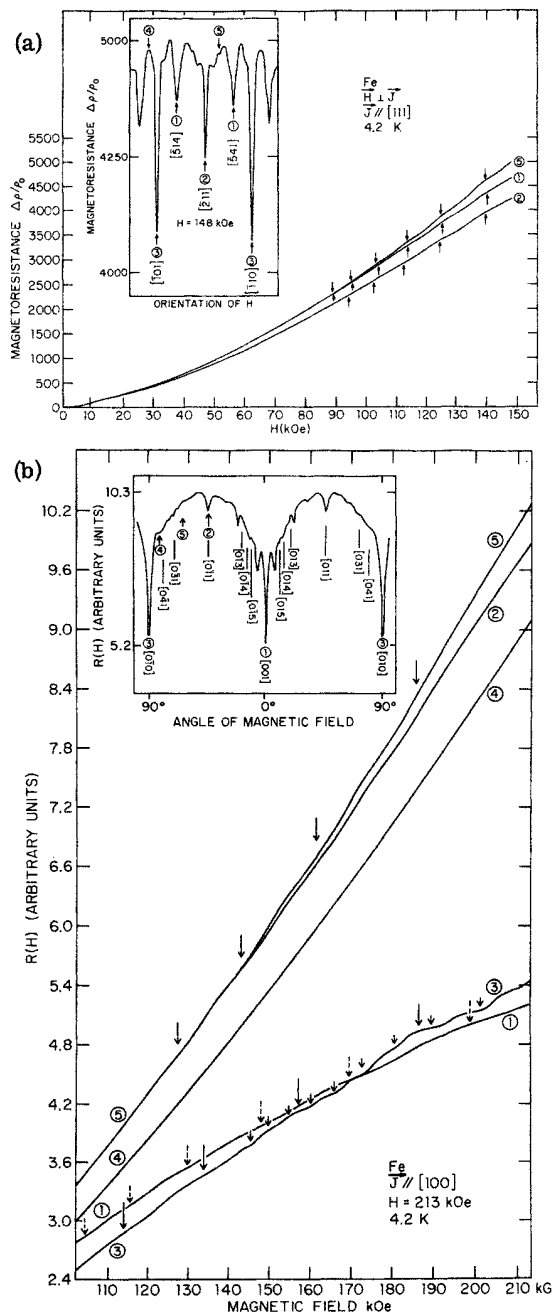


FIG. 7. (a) Field-dependence curves for iron showing Shubnikov-de Haas oscillations corresponding to frequencies of 1.5 MG. Relevant field orientations are specified in the insert. (b) Field-dependence curves for an iron specimen with current slightly off $[100]$. Shubnikov-de Haas oscillations with frequencies of 3 (circled three), 1 and 4.7 MG, 1, 1.3 MG, and 5, 1.4 MG, respectively, are shown for the various field directions indicated on the rotation diagram.

served as shown in curve B of Fig. 8(a). This behavior is observed for an angular field range within $\pm (5^\circ - 10^\circ)$ of the basal plane when the current lies

in the basal plane.

A recent measurement of the magnetoresistance by Batallan and Rosenman²⁴ shows a volcanolike

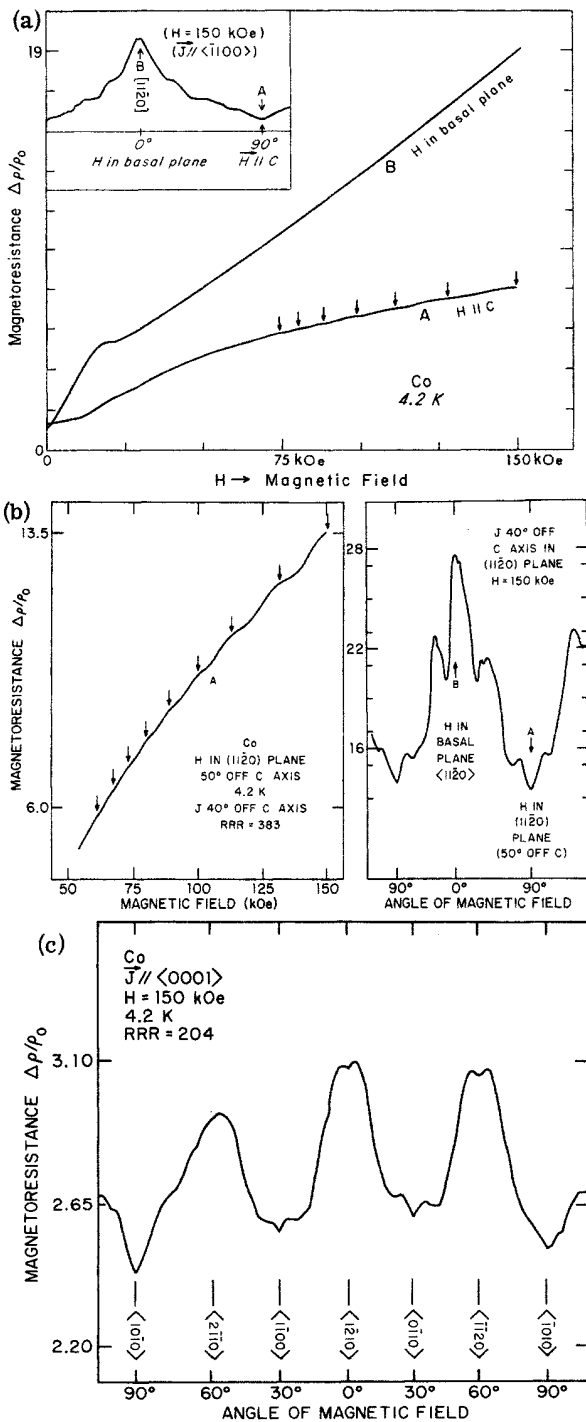


FIG. 8. Transverse magnetoresistance rotation diagrams and field sweeps for cobalt specimens. (a) Current in the basal plane parallel to a $[1100]$ direction. (b) Current in the $(11\bar{2}0)$ plane 40° off the c axis. (c) Current parallel to the c axis.

structure similar to that in Fig. 8(a), but with a greater splitting of the peak at point *B* of the transverse-rotation diagram. For the field direction at the minimum of the splitting corresponding to exact alignment in the basal plane they observe a trend toward saturation while adjacent field directions at approximately $\pm 5^\circ$ from the basal plane show a coefficient $n > 1$ as reported here. It is quite possible that our field orientation was not sufficiently accurate to show this saturation for field and current located exactly in the basal plane. The current axes and a number of the field sweeps used in the present experiments are indicated in the stereo plot of Fig. 9. The current axis for the samples shown here are along $\langle 0001 \rangle$, $\sim 40^\circ$ off $\langle 0001 \rangle$ in the $(11\bar{2}0)$ plane and in the basal plane in the $\langle 10\bar{1}0 \rangle$ direction.

The transverse magnetoresistance in cobalt also shows very low-frequency Shubnikov-de Haas oscillations similar to those observed in iron. These are particularly prominent for field directions near the *c* axis, but have been observed at field directions up to 45° from the *c* axis. A typical example is shown in Fig. 10 which corresponds to a field direction along the *c* axis for which the oscillations are observable over a particularly wide range of field. These oscillations are observed for field values from just above saturation ($H \sim 20$ kOe) to 150 kOe. Longitudinal *c*-axis oscillations of the same frequency are also observed down to fields of less than 10 kOe.

The oscillations in the longitudinal magnetore-

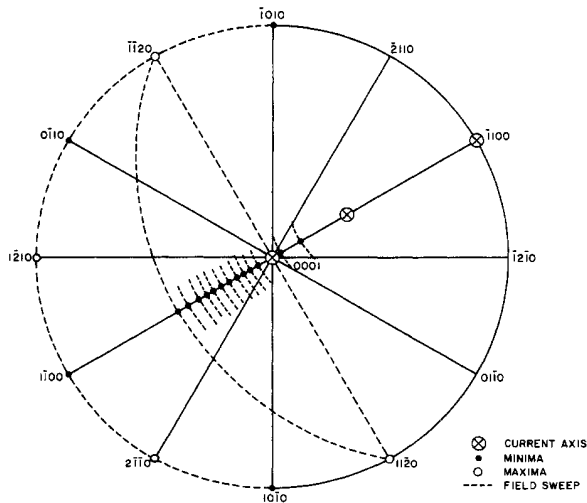


FIG. 9. $\langle 0001 \rangle$ projection plot showing current axes and positions of maxima and minima observed in the transverse rotation curves of cobalt. Successive minima indicated in the $(11\bar{2}0)$ plane were obtained by tipping the crystal with current 40° off *c* axis. The angular dependence of the Shubnikov-de Haas oscillations was measured using these successive field directions.

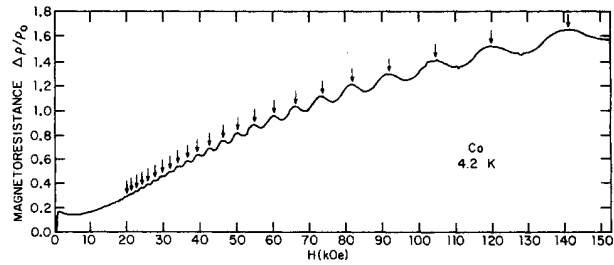


FIG. 10. Shubnikov-de Haas oscillations in cobalt observed for field parallel to the *c* axis the current 40° off the *c* axis in the $(11\bar{2}0)$ plane.

stance can be resolved into more than one frequency and oscillations observed for current and field along the *c* axis are shown in Fig. 11. Three

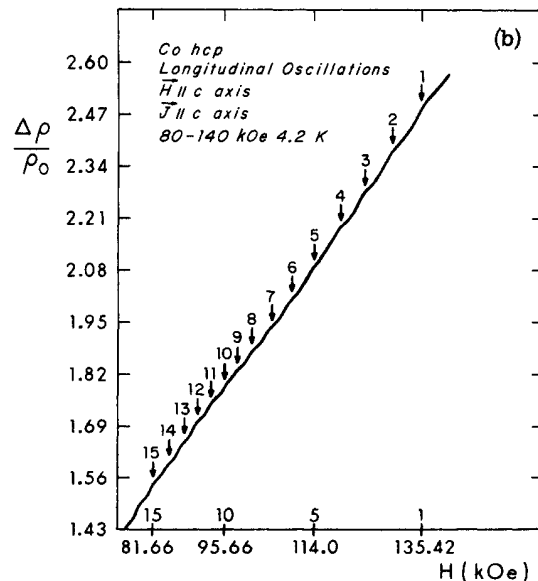
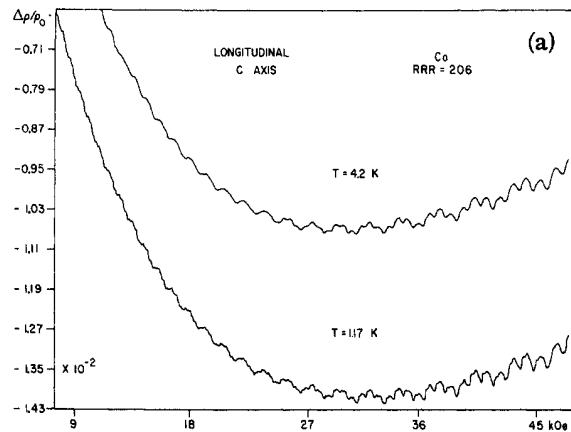


FIG. 11. Longitudinal Shubnikov-de Haas oscillations in cobalt observed with field and current along the *c* axis. (a) Oscillations in field range 0–50 kOe. (b) Oscillations in field range 80–140 kOe.

separate frequencies are resolved in the field range up to 50 kOe, as shown in Fig. 11(a), while the intermediate frequency dominates in the range 50–150 kOe as shown in Fig. 11(b). In the higher-field range there also appears to be a very-long-period oscillation, two periods of which are visible in Fig. 11(b).

The angular dependence of the long-period oscillation has been studied over a range of 65° by tipping one of the specimens in the magnetic field and measuring the field dependence at successive angles ϕ , as indicated in Fig. 9. The field directions are indicated by filled circles and lie in the $(11\bar{2}0)$ plane. The corresponding frequencies have been calculated and are plotted as a function of angle in Fig. 12. The calculated frequencies appear to lie on two separate branches and these are indicated by the solid lines in Fig. 12. The higher-frequency branch is observed for field directions up to 20° from the c axis, while the lower-frequency branch is observed at the larger angles.

IV. DISCUSSION OF RESULTS

A. Iron

The present magnetoresistance results on iron can be compared to the various features of the Fermi-surface topology expected from the band-structure calculations. We first give a brief review of the band-structure results and then discuss the magnetoresistance data in terms of predicted open-orbit directions as well as cross sections which might play a role in the Shubnikov-de Haas oscillations.

The band-structure calculations for ferromagnetic iron suggest a fairly complex multiply connected Fermi surface. Wakoh and Yamashita¹ used a Green's-function method of calculation and made extensive predictions about the topology of the Fermi surface as shown in Figs. 13(b)–13(e). The figures show both the majority-spin (spin-up) (\uparrow) and the minority-spin (spin-down) (\downarrow) sheets of the Fermi surface which were determined by putting 5.1 and 2.9 electrons in the majority- and minority-spin bands, respectively, and then determining the Fermi level for the majority and minority spin separately. Possible open orbits exist on both the majority and minority sheets and these are indicated by the heavy lines with arrows as shown in Figs. 13(b) and 13(e).

Gold *et al.*¹² have recently given an extensive discussion of the Fermi-surface topology resulting from the various band-structure calculations and they have made a comparison between this topology and their de Haas-van Alphen results on iron. Their analysis suggests some modifications of the topology from that predicted by Wakoh and Yamashita and their proposed Fermi-surface cross sec-

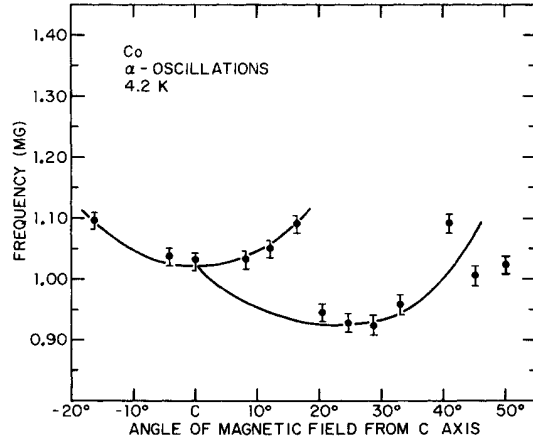


FIG. 12. Angular dependence of low-frequency α oscillations in cobalt. Field is being rotated in the $(11\bar{2}0)$ plane.

tions in the three low-index planes are shown in Fig. 14. One major change indicated by their analysis is a change in the connectivity of the $\langle 110 \rangle$ hole arms on the majority surface along the line HN . These become pinched off near the N point so that open orbits would no longer exist on this sheet alone. The $\langle 110 \rangle$ hole arms then appear as shown in Fig. 13(f). However, Gold *et al.*¹² suggest that contact exists between the $\langle 110 \rangle$ hole arms and the large electron surface of the majority-spin Fermi surface centered on Γ and shown in Fig. 13(d). This point of contact is indicated by the arrow in Fig. 14(a) and could generate open orbits along $\langle 110 \rangle$ directions as well as possibly along $\langle 100 \rangle$ directions. Such bands of open orbits would be very narrow due to the small points of contact. The suggested open orbits reviewed above on both the majority and minority Fermi surfaces involve small points of contact which may in fact be broken by a small gap due to the spin-orbit interaction. The existence of open orbits would then require magnetic breakdown and this would probably occur at relatively low fields and at high fields provide an appreciable section of open Fermi surface. Tawil and Callaway²⁵ have just completed a calculation of the energy bands in ferromagnetic iron and they find arms along the $H-N-H$ line similar to those predicted by Wakoh and Yamashita¹ for the majority-spin Fermi surface. These would support open orbits without magnetic breakdown as shown in Fig. 13(e).

Before discussing the magnetoresistance results in terms of the detailed Fermi-surface topology outlined above, we can make some general comments on the electronic structure based on the observed field dependence of the magnetoresistance. Previous experiments on the magnetoresistance of

iron led to the conclusion that iron was behaving as a compensated metal where compensation indicates an equal number of holes and electrons ($n^e = n^h$). In the case of nonmagnetic metals, Fawcett²⁶ has shown that compensation occurs when the product sZ is even, where s is the number of atoms in the primitive cell and Z is the atomic number. In addition, when the metal is ferromagnetic the metal can be uncompensated even though sZ is even if the quantity n_A is equal to a positive or negative integer where

$$n_A = -\sum_{i^{\uparrow}} n_i^e(\uparrow) - \sum_{i^{\downarrow}} n_i^e(\downarrow) + \sum_{j^{\uparrow}} n_j^h(\uparrow) + \sum_{j^{\downarrow}} n_j^h(\downarrow). \quad (1)$$

The arrows (\uparrow) or (\downarrow) refer to the different spin bands. For iron, $s = 1$ and $Z = 26$ and compensation therefore indicates $n_A = 0$. A more complete discussion of compensation has been given by Fawcett and Reed.²⁷

For a compensated metal in the high-field limit ($\omega_c \tau \gg 1$), the magnetoresistance for a general field

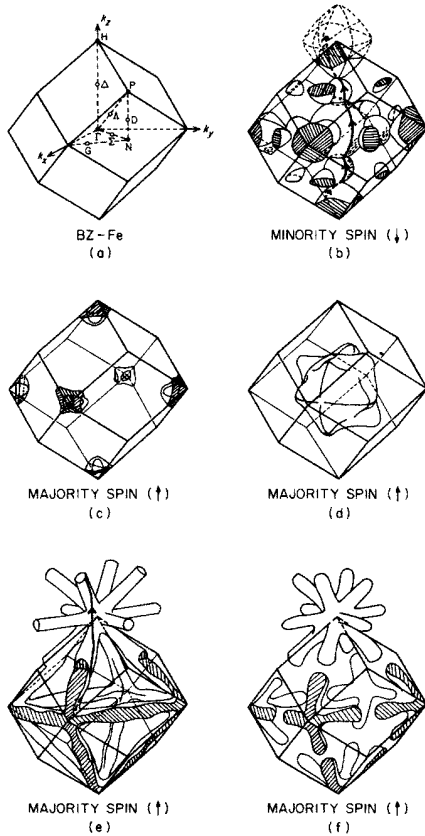


FIG. 13. Fermi surface for iron. (a) Brillouin zone for bcc. (b) Minority-spin Fermi surface. Open orbit along $\langle 100 \rangle$ (after Wakoh and Yamashita, Ref. 1). (c)-(e) Majority-spin Fermi surface (after Wakoh and Yamashita, Ref. 1). (f) Majority-spin hole surface after Gold *et al.*, Ref. 12. This is a modification of the sheet shown in (e).

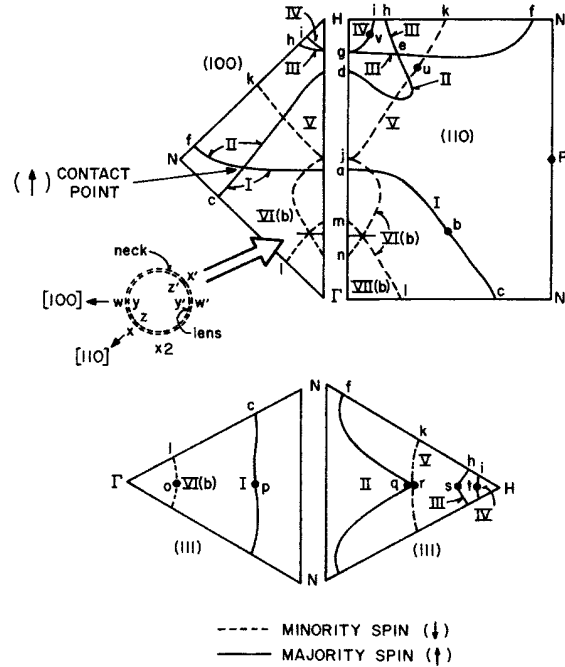


FIG. 14. Fermi-surface cross sections for iron in the three low-index planes (100), (110), and (111) (after Gold *et al.*, Ref. 12).

direction is given by $\Delta\rho/\rho_0 = aB^n$, where $n = 2$. The previous experiments on iron gave values of n approaching 2 at high fields and the present experiments are in agreement with this for applied fields in the range from just above saturation (~ 25 kOe) to approximately 90 kOe. ($B \sim 36\text{--}101$ kG.) If we approximate the magnetoresistance by a two-band model with isotropic masses and relaxation times, then

$$\frac{\Delta\rho}{\rho_0} = \left(\frac{eB}{c}\right)^2 \frac{\tau_e}{m_e} \frac{\tau_h}{m_h} = (\omega_c \tau)_e (\omega_c \tau)_h. \quad (2)$$

If we further assume equal relaxation times for holes and electrons, then $\Delta\rho/\rho_0 = (\omega_c \tau)^2$ and we can estimate an average $\omega_c \tau$ for the present samples which would correspond to some kind of average over all of the electron and hole orbits. For the highest-ratio sample used (see Fig. 2) the values of $(\omega_c \tau)_{av}$ calculated from the magnetoresistance at 35 and 100 kG are 14 and 48, respectively. This would tend to indicate that the high-field limit is reasonably satisfied for most orbits in this field range and one can conclude that most of the carriers are itinerant and that the measured value of n in the range 1.8–1.9 implies compensation. The variation of n with field orientation for general field directions in the same sample and the fact that it is less than 2 may imply the existence of a few cyclotron orbits with heavy masses which are not yet in the high-field limit. The values of n ob-

served here for general field directions are entirely consistent with those observed for nonmagnetic compensated transition metals such as molybdenum and tungsten.²⁸ On the other hand, special field directions corresponding to sharp minima in the rotation diagrams may show lower exponents due to contributions from narrow bands of open orbits which would be expected to reduce the exponent. The effect of open orbits perpendicular to the current on the transverse magnetoresistance of a compensated metal has been estimated by Fawcett and Reed²⁸ to be given by

$$\frac{\rho(B)}{\rho_0} = \frac{t^2}{1 + Dt^2} = \frac{(\omega_c \tau)_{av}^2}{1 + D(\omega_c \tau)_{av}^2}, \quad (3)$$

where $t = (\omega_c \tau)_{av}$ and D is the fraction of the total Fermi surface covered by open orbits. The magnetoresistance would therefore be expected to saturate at a value of $1/D$. If D is a very small fraction, as would generally be expected for iron based on the existing band-structure calculations, then a very high field would be required for saturation if no appreciable breakdown occurs.

Above $B \sim 100$ kG the marked decrease in the exponent n to a range of 1.3–1.5 at $B \sim 160$ kG, as shown in the examples of Figs. 6(a) and 6(b), could be interpreted as indicating the onset of breakdown and an increase in the fraction D of open orbits and hence a more rapid approach to saturation. The further decrease of the exponent n to values less than 1 at minima directions for magnetic induction up to $B \sim 225$ kG substantiates the trend toward saturation and is the expected behavior for open-orbit minima. The analysis is still somewhat complicated, since a decrease in n above 100 kG is observed for all field directions measured and not just at the sharp minima. The breakdown would therefore seem to occur for a range of field directions and interrupt the compensation generally rather than for specific open-orbit directions identified with minima. The breakdown might also involve an electron transition from a spin-up to a spin-down sheet of the Fermi surface which could effect the compensation through the value of n_A . The present experiments do not provide enough information to examine the specific possibilities in detail.

The sharp minima observed in the magnetoresistance rotation diagrams look very similar to the structure expected if open orbits exist in certain specific directions. These minima are observed in applied fields down to 10 kOe although there is a considerable variation in the relative magnitude of the anisotropy as the field is increased over the range up to 150 kOe and, as previously mentioned, the relative depth of various minima can become interchanged as the field is increased above 50 kOe. Reed and Fawcett¹³ were the first to suggest

that the minima observed in iron were consistent with narrow bands of open orbits running parallel to $\langle 100 \rangle$ and $\langle 110 \rangle$ directions. The transverse magnetoresistance due to open orbits will be given by

$$\Delta\rho/\rho_0 = C_1 B^2 \cos^2 \alpha + C_2 \sin^2 \alpha, \quad (4)$$

where α is the angle between the open-orbit direction and the current direction. For the $\langle 100 \rangle$ current axis a transverse field oriented along $\langle 100 \rangle$ and $\langle 110 \rangle$ corresponds to $\alpha = 90^\circ$ for $\langle 100 \rangle$ - and $\langle 110 \rangle$ -directed open orbits, respectively. For the $\langle 110 \rangle$ current axis, the field oriented along $\langle 100 \rangle$ and $\langle 110 \rangle$ corresponds to $\alpha = 90^\circ$ for $\langle 110 \rangle$ - and $\langle 100 \rangle$ -directed open orbits, respectively. For the $\langle 111 \rangle$ current axis, the field oriented along $\langle 112 \rangle$ corresponds to $\alpha = 90^\circ$ for $\langle 110 \rangle$ -directed open orbits. We have not observed saturation up to 150 kOe for any of these minima corresponding to high-symmetry transverse-field directions, but in these cases the symmetry of the Fermi surface may produce interesting sets of open orbits which will cause most orbits to be closed or at most extended over several zones. However, the recent extension of the measurements to 215 kOe does show an approach to saturation ($n < 1$) for several of these low-index minima.

In the tipping experiment with a $\langle 111 \rangle$ current axis the minima observed in the $\{110\}$ planes correspond to $\alpha = 90^\circ$ for $\langle 110 \rangle$ -directed open orbits. However, these minima corresponding to higher-index field directions do not show a greater trend toward saturation than the minima observed for low-index high-symmetry transverse-field directions. Anisotropy in the relative depth of the minima is observed as the $\langle 111 \rangle$ axis is tipped away from the transverse orientation, as shown in Fig. 4. For example, the minima observed for fields in $\{110\}$ and $\{100\}$ planes become deeper as the field approaches the $[001]$ pole. This suggests that the open sections of Fermi surface existing for fields near the $[001]$ pole (see Fig. 5) make a stronger contribution to the magnetoresistance than for field directions in $\{110\}$ planes making large angles with the $[001]$ direction. Further data will be needed to analyze the topology in detail.

In addition to the strong minima for field directions in $\{100\}$ and $\{110\}$ we also see minima corresponding to field directions in $\{410\}$ planes over a limited angular range as indicated by the open triangles in Fig. 5. This would indicate the possible existence of open orbits along $\langle 410 \rangle$ directions. A multiply connected Fermi surface with $\langle 100 \rangle$ - and $\langle 110 \rangle$ -directed sets of open orbits could in principle provide such open-orbit directions either by alternate use of $\langle 100 \rangle$ and $\langle 110 \rangle$ segments or by use of alternate $\langle 100 \rangle$ open directions. This would be most likely for field directions reasonably close to the $\langle 100 \rangle$ pole as is roughly the case in Fig. 5. For

field directions within 15° of the $\langle 100 \rangle$ pole we also observe minima which appear to lie in planes such as the $\{530\}$ and $\{310\}$ and these are indicated by open squares and filled triangles in Fig. 5. It is possible that there are a large number of open-orbit directions surrounding $\langle 100 \rangle$ all constructed from the basic $\langle 100 \rangle$ or $\langle 110 \rangle$ open directions. More detailed measurements will be required to resolve this point.

Open orbits in the $\langle 100 \rangle$, $\langle 110 \rangle$, and $\langle 310 \rangle$ directions have been predicted by Wakoh and Yamashita¹ from their band-structure calculation and it would require only small adjustments of their topology to produce additional open orbits in $\langle 410 \rangle$ and $\langle 530 \rangle$ directions. Minima in $\{110\}$ planes indicated by open circles in Figs. 3 and 5 would correspond to $\langle 110 \rangle$ open orbits along the majority hole arms of Fig. 13(e). Minima in the $\{100\}$ planes indicated by filled circles would correspond to $\langle 100 \rangle$ open orbits along the minority Fermi surface of Fig. 13(b) and the minima in the $\{310\}$ plane indicated by filled triangles would correspond to $\langle 310 \rangle$ open orbits which could be constructed from segments of the $\langle 100 \rangle$ open directions of the minority-spin Fermi surface of Fig. 13(b).

The topology suggested by Gold *et al.*¹² could in principle support a similar set of open orbits and might have additional flexibility due to open directions in both $\langle 110 \rangle$ and $\langle 100 \rangle$ on the majority Fermi surface utilizing the two sheets of Figs. 13(f) and 13(d).

The Shubnikov-de Haas frequencies observed in iron have been compared to the de Haas-van Alphen frequencies observed by Gold *et al.*¹² and at present only a few general comments can be made. The Shubnikov-de Haas frequencies in the range 1–1.5 MG are less than half of the lowest de Haas-van Alphen frequency of 3.85 MG observed by Gold *et al.* and attributed to the lens shown in Fig. 14. It is possible that this lens is much smaller than indicated in Fig. 14, but more data will be necessary before reaching any conclusions. The higher Shubnikov-de Haas frequency of 4.7 MG is fairly close to an observed de Haas-van Alphen frequency of 5.04 MG assigned to the neck indicated in Fig. 14. Initial analysis of the data indicates that this frequency may be field dependent in the range above 150 kOe.

B. Cobalt

The general behavior of the field dependence of magnetoresistance in cobalt reported here indicates that it is an uncompensated metal as was previously concluded by Reed and Fawcett.¹³ Assuming that this is the correct conclusion, then open orbits must exist in the basal plane in order to account for the nonsaturation of magnetoresistance when current and field are both close to the basal plane.

The saturation observed by Batallan and Rosenman²⁴ for field and current exactly in the basal plane would indicate that open orbits may also exist along the c direction and will therefore tend to short out the quadratic contribution from open orbits parallel to the basal plane as the field approaches exact alignment in the basal plane. Such a narrow band of open orbits would exist along the c axis if a narrow neck were present on the majority Fermi surface at the Γ point of the Brillouin zone, as shown in Fig. 15(a). The open orbits parallel to the basal plane would then still account for the values of n greater than 1 observed for field directions at small angles from the basal plane where the open orbits parallel to c are rapidly truncated due to the narrowness of the neck. For current along the c axis and field in the basal plane we observe an exponent $n < 1$. If there were strong contributions from open orbits along c then n should approach 2 unless open orbits also exist parallel to the basal plane. Open orbits parallel to the basal plane could be supported by the minority-spin Fermi surface suggested in Fig. 15(b). The topology necessary

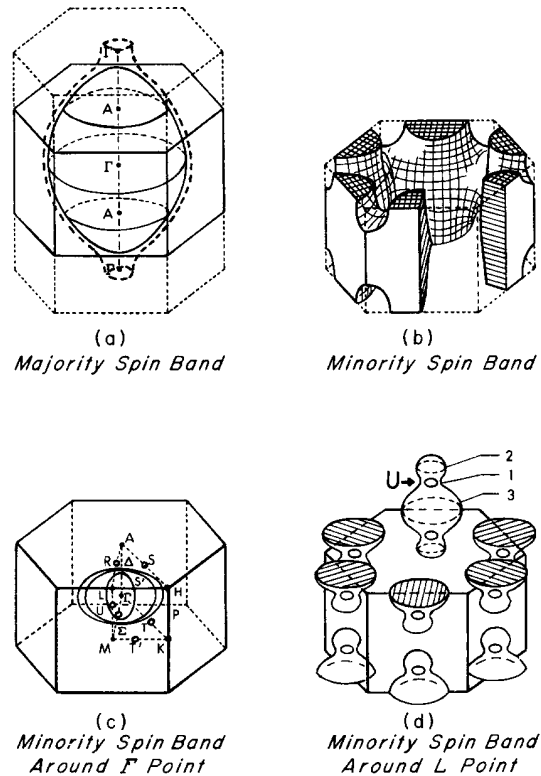


FIG. 15. Fermi surface of cobalt. (a) Majority-spin Fermi surface (after Wakoh and Yamashita, Ref. 10). Dotted line shows modification proposed by Rosenman and Batallan, Ref. 16. (b) and (c) Minority-spin Fermi surface proposed by Wakoh and Yamashita, Ref. 10. (d) Modification of minority Fermi surface around U point proposed in present paper.

to explain the above results might also exist if the majority-spin Fermi surface is multiply connected in the basal plane as well as along the c axis. This point will have to be resolved in further experiments. In addition to these general conclusions we have also made a detailed calculation of the Shubnikov-de Haas frequencies observed and have attempted to identify these with the existence of small sections of the Fermi surface.

Band-structure calculations have been carried out for cobalt by Connolly¹¹ using an augmented-plane-wave method and by Wakoh and Yamashita¹⁰ using a Green's-function method. Wakoh and Yamashita have made the most complete analysis in terms of the possible Fermi-surface topology and their predicted sections of Fermi surface are shown in Fig. 15. The minority-spin band around the L point as shown in Fig. 15(d) has been modified from the original topology of Wakoh and Yamashita. The modified version shown here supports additional extremal orbits labeled 1 and 2. It also provides a strong possibility for breakdown between the small inner lens and the outer-hole surface at the location of orbit 1. Their band-structure calculation was made for paramagnetic cobalt and the spin-up and spin-down Fermi surfaces were obtained by imposing a value of $1.56\mu_B$ per atom on a rigid-band model resulting in an exchange splitting of 1.71 eV. The Fermi surfaces correspond to 10.56 spin-up and 7.44 spin-down electrons per unit cell.

In order to interpret their recent de Haas-van Alphen measurements, Rosenman and Batallan¹⁸ have suggested that the spin-up Fermi surface should be modified as shown by the dashed surface indicated in Fig. 15(a). This corresponds to the presence of a narrow neck at the point Γ and this can be accomplished by adjusting the exchange splitting closer to the experimental value of 1.05 eV found by Eastman²⁹ from photoemission experiments. This neck would also produce a narrow band of open orbits along the c -axis direction as previously mentioned.

The Shubnikov-de Haas oscillations observed in the present experiment have been analyzed by plotting the oscillation number against $1/B$ and determining the period of the oscillation from the slope. The appropriate plots for the longitudinal oscillations of Fig. 10 are shown in Fig. 16 and result in periods of 9.3×10^{-7} , 2.8×10^{-7} , and $0.86 \times 10^{-7} \text{ G}^{-1}$ or frequencies of 1.07, 3.57, and 11.63 MG. The high-field transverse oscillations are on the order of 1 MG in frequency and are probably associated with the same small piece of Fermi surface which gives rise to the 1.07 MG longitudinal oscillation. The transverse oscillations of approximately 1-MG frequency have been studied as a function of field angle in the $(11\bar{2}0)$ plane and the angular dependence

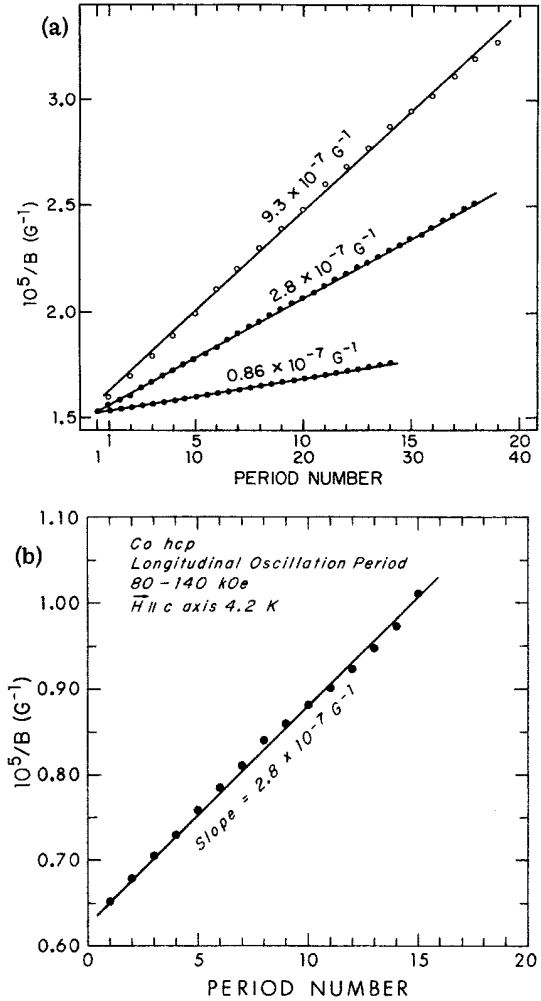


FIG. 16. Plots of longitudinal-oscillation number against $1/B$ for data of Fig. 11; (a) 0-50 kOe, (b) 80-140 kOe.

of the frequency was plotted in Fig. 12. The magnitude and angular variation are very similar to the results for the α oscillations measured in the de Haas-van Alphen experiment of Rosenman and Batallan¹⁶ where two branches are observed as the field is moved away from the c axis in the $(10\bar{1}0)$ plane. In the present magnetoresistance experiment in the $(11\bar{2}0)$ plane the lower branch shows a minimum at $\sim 30^\circ$ as is also the case for the de Haas-van Alphen experiment in the $(10\bar{1}0)$ plane. The magnetoresistance oscillation appears to be associated with only one branch at a time and appears to jump from the upper branch to the lower branch at $\sim 20^\circ$ off the c axis. This jump could be associated with a critical magnetic breakdown point due to the Fermi-surface geometry or to an energy gap which is dependent on field direction. The amplitude of the oscillations shows a considerable

variation with field direction also indicating that breakdown might be playing some role.

The smallest piece of Fermi surface resulting from the band-structure calculation of Wakoh and Yamashita is the small pocket in the minority-spin band (spin down) located at the point U as indicated in Fig. 15(d). This is a very small pocket and its existence is very sensitive to the exact placement of the Fermi level. Whether it is holelike or electronlike depends on the potential used and in the calculation of Wakoh and Yamashita it is holelike. The frequency of 10^6 G corresponds to a radius of the pocket equal to approximately 0.04 of the Brillouin-zone radius or a pocket containing about 10^{-4} electrons per atom. The increase in frequency at angles away from the c -axis direction could be interpreted as indicating that the pocket is elongated along LM rather than in a direction perpendicular to the c axis, as is indicated in the band-structure calculation. However, breakdown to the larger hole surface which closely approaches the pocket at the U point [see Fig. 15(d)] might account for this as well as the jump in frequency from one α branch to the other. In fact breakdown at this point may be a mechanism for enhancing the amplitude of the Shubnikov-de Haas oscillations since this amplitude grows unusually large as one approaches the c -axis direction. This mechanism has been discussed in detail by Falicov and co-workers.^{30,31}

The plot of oscillation number against $1/B$ for the c -axis transverse oscillation of Fig. 10 is shown in Fig. 17. The straight line has been drawn from a least-mean-squares fit of the six-highest-field oscillations, and a small deviation from this straight line is observed for the lowest-field oscillations. This deviation appears to be real and is not a consequence of using an incorrect demagnetizing factor. It may be due to the fact that the internal field is not exactly aligned with the external field in the lower-field range. For example, An-

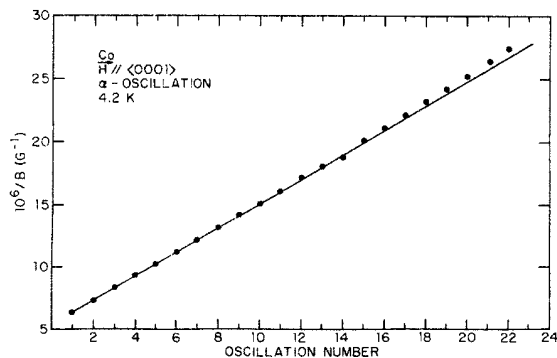


FIG. 17. Plot of oscillation number against $1/B$ for experimental data of Fig. 10.

derson and Hudak¹⁷ have observed a 1.3° change in the direction of \vec{B} over the range 35–54 kOe and this will certainly increase at lower fields.

The intermediate frequency of 3.57 MG observed in the longitudinal magnetoresistance for the field along the c axis corresponds to the β oscillation observed in the de Haas-van Alphen effect by Rosenman and Batallan¹⁶ and by Anderson and Hudak¹⁷ who measured 3.75 and 3.53 MG, respectively. As indicated by the slope in Figs. 16(a) and 16(b), the frequency of this oscillation is independent of field in the range 5–150 kG, although there appears to be a periodic variation at high fields corresponding to a very-long-period oscillation possibly due to magnetic breakdown.

Rosenman and Batallan¹⁶ assign this oscillation to the extremal orbit on the neck of the majority Fermi surface at the Γ point which they suggest is present. They have also made an angular-dependence measurement of the frequency and find that it follows a variation expected for a hyperbolic neck and this is confirmed by Anderson and Hudak.¹⁷ Our measurement is of course consistent with this identification although we have not been able to make an angular-dependence measurement.

In the low-field longitudinal oscillations of Fig. 11 we also observe a frequency equal to 11.63 MG which is not resolved in either the high-field longitudinal- or transverse-magnetoresistance experiments. A similar frequency has also been identified for the field along the c direction in the de Haas-van Alphen experiments and these are referred to as the γ oscillations. Anderson and Hudak¹⁷ have measured two γ oscillations with frequencies $\gamma_1 \approx 11.7$ MG and $\gamma_2 \approx 13.5$ MG. Rosenman and Batallan¹⁶ report a γ oscillation with a frequency of 12.3 MG. At present these oscillations have not been identified with any particular piece of the Fermi surface. The frequency would correspond to a piece with a radius equal to approximately 0.13 of the Brillouin zone radius. Such an orbit might exist on the minority-spin Fermi-surface pockets around the L point as shown in Fig. 15(d) and indicated by the dashed lines labeled 2 or 3. This is a modification of the Fermi surface from that of Wakoh and Yamashita and creates additional extremal areas on the surface around the L point. These extremal areas could be roughly of the right dimension, (~ 0.1 of BZ diameter) although further experiments will be necessary to establish proof of their existence.

Batallan and Rosenman³² have recently reported additional de Haas-van Alphen data on frequencies in the range 9–17 MG and conclude that these are associated with six ellipsoids which are located on the LM line in the Brillouin zone and could therefore coincide with the extremal areas shown in Fig. 15(d).

V. CONCLUSIONS

The magnetoresistance studies of both iron and cobalt show a number of features which can be tentatively identified with features of the Fermi surface topology expected from band-structure calculations. In the case of iron, the magnetoresistance-rotation curves exhibit sharp minima which support the idea of narrow bands of open orbits in a number of directions. The value of the exponent n in the expression $\Delta\rho/\rho_0 = aB^n$ is field dependent above 100 kG and decreases to a value in the range 1.3–1.5 at 160 kG. This decrease has been observed for all field directions measured and suggests that fairly extensive breakdown may be occurring above 100 kG. Preliminary experiments up to 225 kG indicate that n decreases to less than 1 for a number of field directions corresponding to minima. The lower-field behavior is essentially in agreement with that expected for a compensated metal. Low-frequency Shubnikov-de Haas oscillations have been observed corresponding to frequencies in a range 1–1.5 MG and are present for a range of field directions. This frequency range corresponds to a small pocket of the Fermi surface with an extremal area equal to less than one-half that responsible for the lowest observed de Haas-van Alphen frequency of 3.85 MG. A higher-frequency Shubnikov-de Haas oscillation has also been observed for iron in fields from 150 to 215 kOe. The measured frequency of 4.7 MG is close to an observed de Haas-van Alphen frequency of 5.04 MG.

The field dependence of magnetoresistance in cobalt is consistent with the behavior of an uncompensated metal with open orbits existing for certain specific field directions. Nonsaturation of the magnetoresistance is observed for current in the basal plane and field directions within a few degrees of the basal plane suggesting open orbits with directions in the basal plane. Possible open orbits might also exist along the c axis, but all field directions appear to saturate above 100 kOe when current is along the c axis and fields are in the basal plane. If open orbits do exist along the c axis, then open orbits parallel to the basal plane must also exist in order to explain saturation when current is along the c axis and field is in the basal plane. Intersecting sets of open orbits existing on the majority-spin Fermi surface when field is exactly in the basal plane might also explain the results, but real evidence for this is lacking at present.

Large-amplitude Shubnikov-de Haas oscillations have been observed in cobalt with frequencies of 1.07, 3.57, and 11.63 MG for field along the c axis. The angular dependence of the low-frequency α oscillation has been studied over a range of 45° from the c axis in the $\langle 11\bar{2}0 \rangle$ plane and appears to

have a dependence in general agreement with results from de Haas-van Alphen measurements. Two branches are observed but the second branch is observed only for field angles greater than 20° from the c axis. We suggest that the switch from the higher- to the lower-frequency branch at 20° might be due to the existence of breakdown for angles near the c axis which could occur between the small lens at the U point and the larger surrounding hole surface. For angles greater than 20° this breakdown could cease with a consequent reduction in the extremal area of the orbit. The higher-frequency oscillations are consistent with other features of the predicted Fermi surface topology, but no definite assignments can be made at this time.

The experiments to date clearly establish only a few small pieces of the Fermi surface and allow some speculation about the correctness of the existing Fermi-surface calculations and expected open-orbit directions. In the case of iron the samples are reasonably well into the high-field limit, but clearly higher fields and higher purity would lead to additional resolution of the Fermi-surface topology. In the case of cobalt the samples are not pure enough to reach much above the condition $\omega_c\tau \approx 1$ at the highest field and for orbits with large masses this condition is far from satisfied. We clearly do not see the existence of orbits on large sheets of the Fermi surface or additional frequencies due to possible magnetic breakdown between various spin-up and spin-down sections of the Fermi surface. Larger orbits as well as possible orbits arising from spin flips are indicated in Fig. 18.

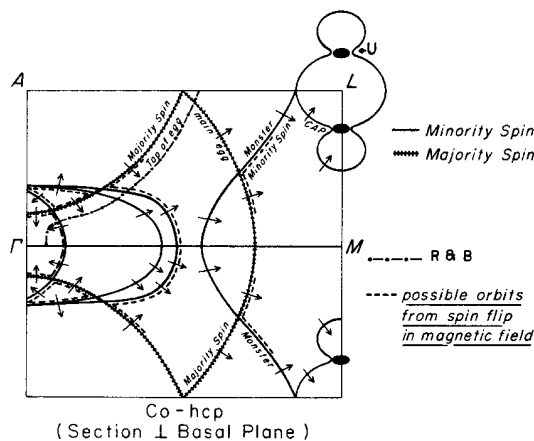


FIG. 18. Cross sections of Fermi surface of cobalt in the plane perpendicular to the basal plane containing the Γ , A , L , M , and U points. Possible additional orbits from spin-flip transitions are indicated. Modification of majority-spin Fermi surface proposed by Rosenman and Batallan is indicated by dot-dashed line.

ACKNOWLEDGMENTS

The authors would like to thank Professor Leo Falicov for a continuing interest in this work and for many stimulating discussions. Professor Vittorio Celli has also contributed many helpful discussions. The authors would like to thank Brenda Young for help in analysis of the data and Werner Frewer for construction of some of the

apparatus. The late Philipp Sommer designed and built many of the sample holders which were essential to the success of the experiment. They would also like to recognize the contribution of Dr. James Beitchman and Douglas Marker who participated in the early phases of this work. Larry Rubin and his group have contributed to the success of the experiments at the Francis Bitter National Magnet Laboratory.

*Work supported by U. S. Atomic Energy Commission Contract No. (AT-40)-3105 at University of Virginia, NSF No. Grant GP-21312 at Massachusetts Institute of Technology, and NSF No. GH-35690 at University of Nebraska.

†Work above 80 kOe was performed while the authors were Guest Scientists at the Francis Bitter National Magnet Laboratory, which is supported at M.I.T. by the National Science Foundation.

‡Present address.

¹S. Wakoh and J. Yamashita, *J. Phys. Soc. Jap.* **21**, 1712 (1966).

²K. J. Duff and T. P. Das, *Phys. Rev. B* **1**, 192 (1971).

³M. F. Manning, *Phys. Rev.* **63**, 190 (1943).

⁴J. Callaway, *Phys. Rev.* **99**, 500 (1955).

⁵F. Stern, *Phys. Rev.* **116**, 1399 (1959).

⁶J. H. Wood, *Phys. Rev.* **126**, 517 (1962).

⁷L. F. Mattheiss, *Phys. Rev.* **134**, A970 (1964).

⁸E. Abate and M. Asdente, *Phys. Rev.* **140**, A1303 (1965); *Phys. Rev.* **185**, 861 (E) (1969).

⁹R. Maglic and F. M. Mueller, *Int. J. Mag.* **1**, 289 (1971).

¹⁰S. Wakoh and J. Yamashita, *J. Phys. Soc. Jap.* **28**, 1151 (1970).

¹¹J. W. D. Connolly, *Int. J. Quantum Chem.* **11S**, 257 (1968).

¹²A. V. Gold, L. Hodges, P. T. Panousis, and D. R. Stone, *Int. J. Magn.* **2**, 357 (1971).

¹³W. A. Reed and E. Fawcett, *Phys. Rev.* **136**, A422 (1964).

¹⁴*International Conference on Magnetism, Nottingham* (The Institute of Physics and the Physical Society, London, 1965), p. 120.

¹⁵Acar Isin and R. V. Coleman, *Phys. Rev.* **137**, A1609 (1965).

¹⁶I. Rosenman and F. Batallan, *Phys. Rev. B* **5**, 1340 (1971).

¹⁷J. R. Anderson and J. J. Hudak, *AIP Conf. Proc.* **5**, 477 (1972); *AIP Conf. Proc.* **10**, 46 (1973).

¹⁸D. L. Marker, J. W. Reichardt, and R. V. Coleman, *J. Appl. Phys.* **42**, 1338 (1971).

¹⁹R. V. Coleman, *Metall. Rev.* **9**, 261 (1964).

²⁰S. S. Brenner, *The Art and Science of Growing Crystals*, edited by J. J. Gilman (Wiley, New York, 1963), Chap. 2, p. 30.

²¹S. S. Brenner, *Acta Metall.* **4**, 62 (1956).

²²P. W. Shumate, Jr., R. V. Coleman, and R. C. Fivaz, *Phys. Rev. B* **1**, 394 (1970).

²³E. Fawcett (private communication).

²⁴F. Batallan and I. Rosenman, *Solid State Commun.* **12**, 75 (1973).

²⁵R. A. Tawil and J. Callaway, *Phys. Rev. B* (to be published).

²⁶E. Fawcett, *Phys. Rev.* **128**, 154 (1962).

²⁷E. Fawcett and W. A. Reed, *Phys. Rev.* **131**, 2463 (1963).

²⁸E. Fawcett and W. A. Reed, *Phys. Rev.* **134**, A723 (1964).

²⁹D. O. Eastman, *J. Appl. Phys.* **40**, 1387 (1969).

³⁰L. M. Falicov and Paul R. Sievert, *Phys. Rev.* **138**, A88 (1965).

³¹L. M. Falicov, A. B. Pippard, and Paul R. Sievert, *Phys. Rev.* **151**, 498 (1966).

³²F. Batallan and I. Rosenman, Thirteenth International Conference on Low Temperature Physics (unpublished).